

Appendix 1: The inclusion and exclusion criteria

The inclusion criteria were as follows:

- (I) Patients with pathological diagnosis of NPC;
- (II) NPC patients in the locoregionally advanced stage (III–IVa) based on the 8th edition of the International Union Against Cancer/American Joint Committee on Cancer staging system;
- (III) Patients who received IC and concurrent chemoradiotherapy;
- (IV) Clinical data (including follow-up information) and nasopharyngeal MR images of the patient before treatment were complete.

The exclusion criteria were as follows:

- (I) Unmeasured (<5 mm) primary NPC tumor;
- (II) Lack of clinical data or MR images before treatment;
- (III) MR images with insufficient quality;
- (IV) Antineoplastic therapy was administered before MR examination;
- (V) Pre-existing or concurrent other primary malignant tumors.

Appendix 2: Detailed MR scanning protocols and acquisition parameters

Hospital I (Guangxi Medical University Cancer Hospital)

Patients were examined using a 3.0T MRI scanner (GE Healthcare Discovery MR750, USA). T₂WI and CET₁WI were obtained. The parameters were listed as follows: T₂WI (TR =6,760 ms, TE =91 ms), CET₁WI (TR =957 ms, TE =19 ms), matrix size =256×256, FOV =240 mm × 240 mm, slice thickness =5 mm, flip angle =90°, and slice spacing =1.0 mm. The contrast agent administered was Gd-DTPA (Magnevist meglumine, Bayer Health Care Pharmaceuticals, Berlin, Germany), which was given at a dose of 0.1 mmol/kg body weight (flow rate: 2.0 mL/sec).

Hospital II (Wuzhou Red Cross Hospital)

Patients were examined using a 3.0T MRI scanner (Magnetom Skyra, Siemens Healthcare, Germany). T₂WI and CET₁WI were obtained. The parameters were listed as follows: T₂WI (TR =3,500 ms, TE =95 ms), CET₁WI (TR =600 ms, TE =11 ms), matrix size =240×320, FOV =230 mm × 230 mm, slice thickness =5 mm, flip angle =90°, and slice spacing =0.5 mm. The contrast agent administered was Gd-DTPA (Magnevist meglumine, Bayer Health Care Pharmaceuticals), which was given at a dose of 0.1 mmol/kg body weight (flow rate: 2.0 mL/sec).

Hospital III (The Second Affiliated Hospital of Guangxi Medical University)

Patients were examined using a 3.0T MRI scanner (GE Healthcare Discovery MR750). T₂WI and CET₁WI were obtained. The parameters were listed as follows: T₂WI (TR =7,061 ms, TE =68 ms), CET₁WI (TR =643 ms, TE =11 ms), matrix size =288×192, FOV =220 mm × 220 mm, slice thickness =4 mm, flip angle =111°, and slice spacing = 0.4 mm. The contrast agent administered was Gd-DTPA (Magnevist meglumine, Bayer Health Care Pharmaceuticals), which was given at a dose of 0.1 mmol/kg body weight (flow rate: 2.0 mL/sec).

Appendix 3: The XGBoost algorithm

The XGBoost is a relatively new ensemble learning algorithm that has been widely used in classification and regression tasks, but its application in prognostic analysis is relatively limited. It enhances traditional gradient boosting by using Newton's method to solve for the loss function extremes, utilizing the second-order Taylor expansion of the loss function, and introducing a regularization term. The training objective of the XGBoost model consists of two components: the loss function derived from gradient boosting and a regularization term. The principle of the XGBoost algorithm can be succinctly

summarized as follow, it operates on a feature vector, assigning it a corresponding output, y_i :

$$y_i = \sum_{k=1} K f_k(x_i), f_k \in F \quad [1]$$

In this study, by incorporating a Cox loss function into the XGBoost algorithm, we successfully developed a prognostic machine learning model suitable for survival data to predict PFS in LANPC patients. During the model training phase, we fine-tuned the hyperparameters using grid search to optimize model performance. In addition, the Harrell C-index was used as the primary evaluation metric to assess model performance across the training cohort and multiple validation cohorts. The optimal hyperparameter configuration was determined according to the comprehensive performance of the model in the training, internal validation, and external validation cohorts.

Appendix 4: The SHAP algorithm

The SHAP packages (<https://github.com/slundberg/shap>) provides utilities for calculating Shapley values for a variety of machine learning algorithms, and is optimized for tree-based algorithms such as XGBoost and GBM. Shapley values come from classical game theory, and are the only additive feature attribution method that yield the combination of local accuracy, consistency, and allowance for missingness. The SHAP formula is as follows:

$$g(z') = \varnothing_0 + \sum_{i=1}^M \varnothing_i z'_i \quad [2]$$

where g is the explanation model, M is the number of simplified input features, $\varnothing_i \in \mathcal{R}$ is the feature attribution for a feature i , $z' \in \{0,1\}^M$, and \varnothing_0 represents the model output with all the simplified inputs missing. The z'_i variables typically represent a feature being observed ($z'_i = 1$) or unknown ($z'_i = 0$).

Table S1 The hyperparameters of the combined XGBoost survival model

Parameters	Type	Explanation	Values
Objective	String	Specify the learning task and the corresponding learning objective	'survival:cox'
Booster	String	Specify which booster to use: gbtree, gblinear or dart	'gbtree'
Max_depth	Int	Maximum tree depth for base learners	3
N_estimators	Int	Number of boosted trees to fit	7
Alpha	Float	L1 regularization term on weights	0.001
Lambda	Float	L2 regularization term on weights	0.00001
Gamma	Float	Minimum loss reduction required to make a further partition on a leaf node of the tree	1
Min_child_weight	Float	Minimum sum of instance weight (hessian) needed in a child	2
Colsample_bytree	Float	Construct the subsample ratio for each tree column	0.5
Subsample	Float	The subsample ratio of the training instance	0.3
Eta	Float	Used in updates to prevent over-fitting step size shrinkage	0.3

XGBoost, eXtreme Gradient Boosting.

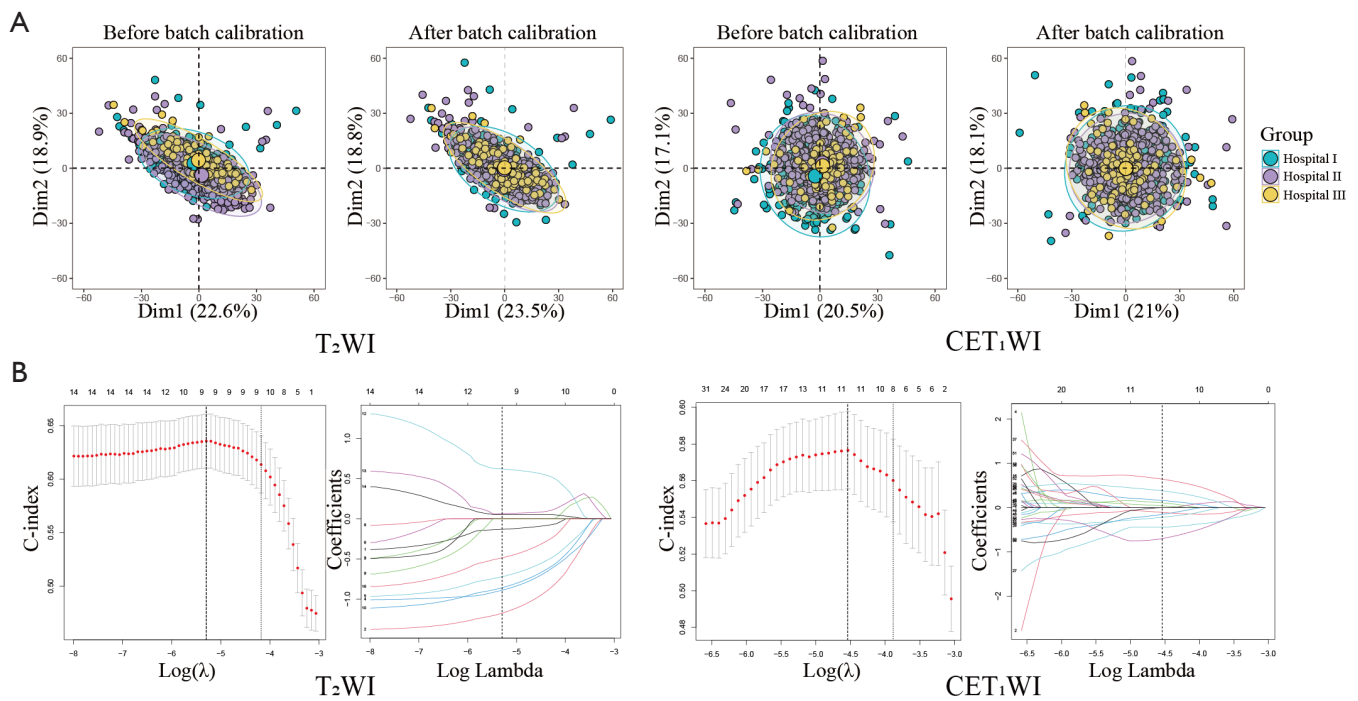


Figure S1 Removal of batch effects and radiomics feature selection. (A) Remove batch effect. The Combat harmonization algorithm was utilized to pool the radiomics data of MRI from different hospitals. Principal component analysis was employed for dimensionality reduction, and the first two principal components of radiomics features were visualized in a two-dimensional scatter plot. The X- and Y-axis represent the two principal component dimensions. The data were well-corrected after performing Combat. (B) Radiomics feature selection. The LASSO model employed a 10-fold cross-validation technique to determine the optimal tuning parameter (λ) based on the minimum criteria. Hospital I: Guangxi Medical University Cancer Hospital; hospital II: Wuzhou Red Cross Hospital; hospital III: The Second Affiliated Hospital of Guangxi Medical University. C-index, concordance index; CET₁WI, contrast-enhanced T₁-weighted imaging; LASSO, least absolute shrinkage and selection operator; MRI, magnetic resonance imaging; T₂WI, T₂-weighted imaging.

Table S2 Univariate Cox analysis of the most predictive radiomics features from T₂WI and CET₁WI

Sequence	Filter	Type	Feature name	HR (95% CI)	P value
T ₂ WI	Wavelet.HLH	GLRLM	GrayLevelNonUniformityNormalized	0.317 (0.109–0.916)	0.034
	Wavelet.LLH	GLDM	DependenceVariance	0.423 (0.207–0.867)	0.019
	Wavelet.LHL	GLCM	MCC	0.446 (0.210–0.948)	0.036
	Original	Shape	Flatness	0.466 (0.240–0.905)	0.024
	Original	Shape	Elongation	0.499 (0.261–0.953)	0.035
	Wavelet.LLL	GLCM	Imc1	0.524 (0.276–0.996)	0.049
	Wavelet.HHL	GLSZM	LargeAreaEmphasis	2.427 (1.281–4.600)	0.007
	Wavelet.HHL	GLSZM	ZoneVariance	2.429 (1.281–4.605)	0.007
	Wavelet.HHL	GLSZM	LargeAreaLowGrayLevelEmphasis	2.508 (1.301–4.835)	0.006
CET ₁ WI	Wavelet.LHL	GLRLM	RunEntropy	0.342 (0.166–0.706)	0.004
	Wavelet.LHL	GLSZM	SmallAreaEmphasis	0.386 (0.195–0.764)	0.006
	Wavelet.LHH	Firstorder	Maximum	0.422 (0.189–0.942)	0.035
	Wavelet.LHL	NGTDM	Strength	0.423 (0.184–0.972)	0.043
	Wavelet.LHH	GLDM	DependenceEntropy	0.462 (0.229–0.934)	0.031
	Wavelet.LHL	GLDM	LowGrayLevelEmphasis	1.944 (1.010–3.739)	0.046
	Wavelet.LLL	Firstorder	Mean	2.166 (1.017–4.613)	0.045
	Original	GLCM	InverseVariance	2.195 (1.063–4.532)	0.034
	Wavelet.HHH	Firstorder	Minimum	2.261 (1.013–5.047)	0.046
Wavelet.HHL	GLCM	Imc1	2.605 (1.204–5.634)	0.015	

CET₁WI, contrast-enhanced T₁-weighted imaging; CI, confidence interval; GLCM, gray level co-occurrence matrix; GLDM, gray level dependence matrix; GLRLM, gray level run length matrix; GLSZM, gray level size zone matrix; HR, hazard ratio; NGTDM, neighboring gray tone difference matrix; T₂WI, T₂-weighted imaging.

Table S3 Inter- and intra-class correlation coefficients of T₂WI sequence modeling features

Radiomics features	Inter-class correlation coefficient (95% CI)	Intra-class correlation coefficient (95% CI)
T ₂ WI_original_shape_Elongation	0.89 (0.87–0.93)	0.94 (0.89–0.96)
T ₂ WI_original_shape_Flatness	0.91 (0.88–0.95)	0.91 (0.85–0.95)
T ₂ WI_wavelet-LLH_gldm_DependenceVariance	0.90 (0.87–0.94)	0.99 (0.98–0.99)
T ₂ WI_wavelet-LHL_gldm_MCC	0.90 (0.85–0.94)	0.92 (0.87–0.95)
T ₂ WI_wavelet-HLH_gldm_GrayLevelNonUniformityNormalized	0.90 (0.86–0.94)	0.99 (0.98–1.00)
T ₂ WI_wavelet-HHL_glszm_LargeAreaEmphasis	0.91 (0.86–0.93)	0.93 (0.88–0.96)
T ₂ WI_wavelet-HHL_glszm_LargeAreaLowGrayLevelEmphasis	0.90 (0.87–0.94)	0.94 (0.90–0.97)
T ₂ WI_wavelet-HHL_glszm_ZoneVariance	0.89 (0.84–0.93)	0.93 (0.88–0.96)
T ₂ WI_wavelet-LLL_gldm_lmc1	0.89 (0.85–0.93)	0.93 (0.88–0.96)

CI, confidence interval; T₂WI, T₂-weighted imaging.

Table S4 Inter- and intra-class correlation coefficients of CET₁WI sequence modeling features

Radiomics features	Inter-class correlation coefficient (95% CI)	Intra-class correlation coefficient (95% CI)
CET ₁ WI_original_gldm_InverseVariance	0.91 (0.88–0.95)	0.99 (0.98–0.99)
CET ₁ WI_wavelet-LHL_gldm_LowGrayLevelEmphasis	0.91 (0.89–0.95)	0.98 (0.98–0.99)
CET ₁ WI_wavelet-LHL_gldm_RunEntropy	0.93 (0.88–0.96)	0.99 (0.98–0.99)
CET ₁ WI_wavelet-LHL_glszm_SmallAreaEmphasis	0.89 (0.85–0.94)	0.97 (0.94–0.98)
CET ₁ WI_wavelet-LHL_ngtdm_Strength	0.90 (0.87–0.94)	0.99 (0.99–1.00)
CET ₁ WI_wavelet-LHH_firstorder_Maximum	0.91 (0.86–0.95)	0.97 (0.95–0.98)
CET ₁ WI_wavelet-LHH_gldm_DependenceEntropy	0.89 (0.87–0.94)	0.98 (0.97–0.99)
CET ₁ WI_wavelet-HHL_gldm_lmc1	0.90 (0.86–0.94)	0.92 (0.87–0.95)
CET ₁ WI_wavelet-HHH_firstorder_Minimum	0.91 (0.85–0.95)	0.99 (0.99–1.00)
CET ₁ WI_wavelet-LLL_firstorder_Mean	0.90 (0.87–0.94)	0.98 (0.97–0.99)

CET₁WI, contrast-enhanced T₁-weighted imaging; CI, confidence interval.

Table S5 Prognostic performance of radiomics models

Models	Training cohort		Internal validation cohort		External validation cohort	
	C-index (95% CI)	P value	C-index (95% CI)	P value	C-index (95% CI)	P value
TNM XGBoost	0.545 (0.495–0.595)	<0.001	0.542 (0.459–0.625)	0.051	0.590 (0.417–0.763)	0.632
T ₂ WI XGBoost	0.676 (0.629–0.723)	0.040	0.646 (0.566–0.726)	0.762	0.626 (0.461–0.791)	0.811
CET ₁ WI XGBoost	0.668 (0.621–0.715)	0.009	0.648 (0.579–0.717)	0.773	0.653 (0.508–0.798)	0.970
Dual-sequence Cox	0.682 (0.637–0.727)	0.018	0.462 (0.380–0.543)	0.068	0.482 (0.304–0.660)	0.127
Dual-sequence XGBoost	0.743 (0.700–0.786)	Ref.	0.663 (0.586–0.740)	Ref.	0.657 (0.485–0.829)	Ref.

C-index, concordance index; CET₁WI, contrast-enhanced T₁-weighted imaging; CI, confidence interval; ref., reference; T₂WI, T₂-weighted imaging; TNM, tumor-node-metastasis; XGBoost, eXtreme Gradient Boosting.

Table S6 Univariate and multivariate Cox regression analyses

Characteristics	Univariate analysis		Multivariate analysis	
	HR (95% CI)	P value	HR (95% CI)	P value
IC	1.906 (1.327–2.737)	<0.001	1.823 (1.264–2.629)	0.001
Sex	1.060 (0.702–1.601)	0.781		
Age	1.002 (0.986–1.018)	0.826		
History	1.041 (0.562–1.931)	0.897		
Smoke	1.354 (0.912–2.008)	0.132		
BMI	0.966 (0.915–1.021)	0.219		
T stage (1–2 vs. 3–4)	1.096 (0.742–1.619)	0.646		
N stage (0–1 vs. 2–3)	1.542 (0.901–2.640)	0.114		
WHO type (I–II vs. III)	1.968 (0.626–6.182)	0.246		
WBC	0.929 (0.855–1.009)	0.079		
Hemoglobin	0.995 (0.984–1.005)	0.330		
Platelet	1.001 (0.999–1.003)	0.366		
Neutrophil	0.910 (0.824–1.005)	0.062		
NLR	0.847 (0.665–1.078)	0.178		
EBV-DNA	1.544 (1.084–2.199)	0.016	1.429 (1.001–2.043)	0.0499
Albumin	1.012 (1.006–1.018)	<0.001	1.012 (1.006–1.018)	<0.001

BMI, body mass index; CI, confidence interval; EBV, Epstein-Barr virus; HR, hazard ratio; IC, induction chemotherapy; NLR, neutrophil lymphocyte ratio; WBC, white blood cell; WHO, World Health Organization.

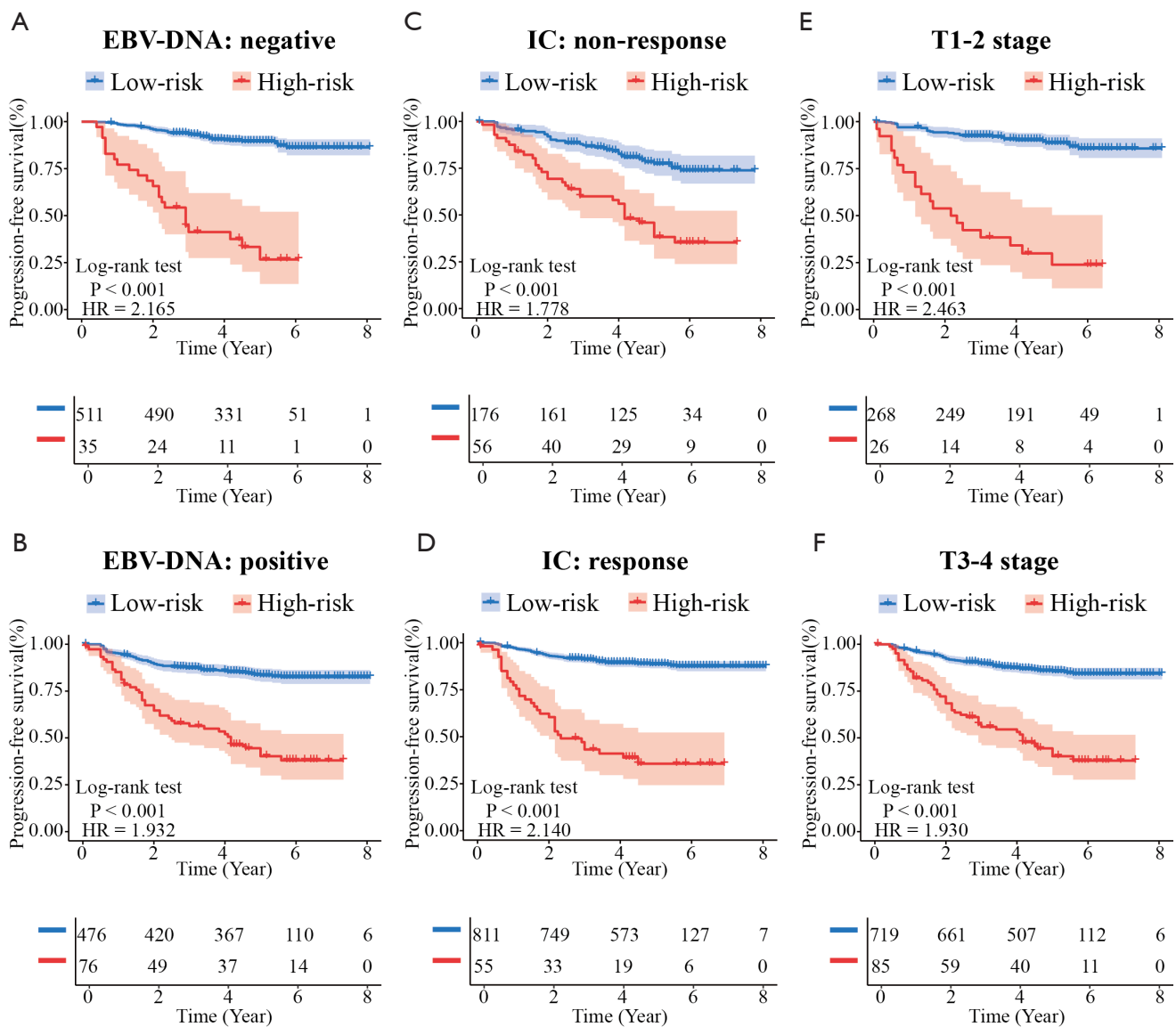


Figure S2 Prognostic subgroup analysis. Stratified Kaplan-Meier analyses were performed to estimate PFS in various subgroups of the pooled cohort, which integrates the training, internal, and external validation cohorts. In the subgroups stratified by EBV-DNA (A,B), IC (C,D), T stage (E,F), patients in the high-risk group exhibited significantly lower PFS than those in the low-risk group (all log-rank $P < 0.01$). The blue and red curves represent the PFS of the low- and high-risk groups, respectively. EBV, Epstein-Barr virus; HR, hazard ratio; IC, induction chemotherapy; PFS, progression-free survival.

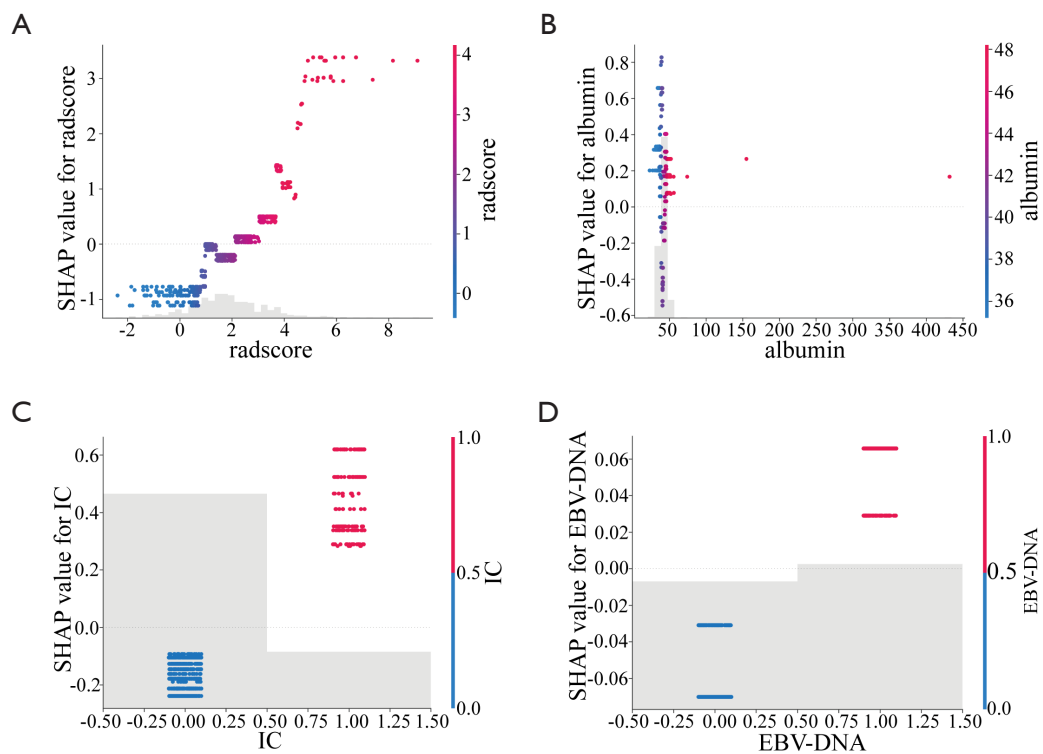


Figure S3 SHAP dependence scatter plot. The relationship between radscore (A), albumin (B), IC (C), and EBV-DNA (D) and PFS in LANPC patients. The X-axis represents the feature value, and the Y-axis represents the SHAP value of the same feature. Vertical dispersion of the data points represents interaction effects. EBV, Epstein-Barr virus; LANPC, locally advanced nasopharyngeal carcinoma; IC, induction chemotherapy; PFS, progression-free survival; radscore, radiomics score; SHAP, SHapley Additive explanation.